Threshold photoemission magnetic circular dichroism at the spin-reorientation transition of ultrathin epitaxial Pt/Co/Pt(111)/W(110) films

K. Hild,* J. Emmel, G. Schönhense, and H. J. Elmers
Institut für Physik, Johannes Gutenberg-Universität, D-55099 Mainz, Germany
(Received 18 September 2009; revised manuscript received 17 November 2009; published 30 December 2009)

We report on the observation of threshold photoemission magnetic circular dichroism (TPMCD) in one-photon photoemission (1PPE) and two-photon photoemission (2PPE) at a Pt-capped ultrathin Co wedge grown on Pt(111)/W(110) using femtosecond laser light. TPMCD measurements result in asymmetries continuously increasing with the sample thickness. This indicates that the TPMCD asymmetry is dominantly influenced by the Co bulk properties. At 5 monolayers (ML) asymmetry values of 0.07% for 1PPE and 0.11% for 2PPE are derived. The spin-reorientation transition is detected at a Co thickness of 5.5 ML. For the perpendicularly saturated sample the TPMCD does not depend on the orientation of the easy axis. Kerr ellipticities and rotations are measured and compared with the TPMCD data in the framework of optical transfer-matrix calculations. The observed TPMCD asymmetry considerably deviates from the behavior of the complex Kerr angle. Moreover, the TPMCD measurements are referred to Co bulk band-structure calculations and the influence of a capping layer on the TPMCD asymmetry is discussed.

DOI: 10.1103/PhysRevB.80.224426 PACS number(s): 79.60.Dp, 75.70.−i, 71.20.Be

I. INTRODUCTION

Magnetic circular dichroism (MCD) is nowadays widely used for the investigation of magnetic properties of surfaces and thin films. Except for synchrotron-based x-ray magnetic circular dichroism (XMCD) methods, one usually observes very small asymmetries for threshold photoemission magnetic circular dichroism (TPMCD) and threshold photoemission magnetic linear dichroism (TPMLD) using visible light.[1,2] Only recently, much larger values were reported:[3–7] a study on a perpendicularly magnetized 12 monolayers (ML) Ni film on Cu(001) revealed MCD asymmetries larger than 10% in threshold photoemission, where the photon energy just exceeds the sample work function.[3] This is remarkable since MCD in the visible-light region suffers from the absence of discrete atomic levels with a high spin-orbit coupling like it is the case in XMCD measurements. Still there is only little knowledge about thin-film systems with high TPMCD asymmetries, the behavior of asymmetries in dependence of the magnetic anisotropy, sample thickness, or capping layers.

Nakagawa and Yokoyama[3] observed a drastic change in the TPMCD asymmetry as a function of the thickness of a wedged Ni film grown on Cu(001). The in-plane magnetized film thicknesses up to the spin-reorientation transition (SRT) at 8 ML showed one order of magnitude smaller asymmetry values in a longitudinal setup than the out-of-plane magnetized regions, starting from 8 ML in a polar setup. Since it can be argued that threshold photoemission magnetic circular dichroism can be treated as a magneto-optical phenomenon[3,8] this behavior corresponds to similar differences between the longitudinal and polar Kerr effect crossing the SRT with increasing sample thickness. The measurements on Ni raise the question whether the TPMCD asymmetry of a completely saturated sample increases continuously from the ultrathin end of the wedge up to higher thicknesses, indicating that surface effects do not play a dominant role. Otherwise a saturation of the TPMCD asymmetry at a few ML of the magnetic film should be observed. Furthermore it might be of interest, if the TPMCD asymmetry is influenced by the orientation of the magnetization easy axis.

In this paper we present TPMCD measurements on a Pt-capped, wedged Co sample grown on Pt(111)/W(110) to investigate the influence of magnetic anisotropy and sample thickness on the TPMCD asymmetries in one-photon photoemission (1PPE) and two-photon photoemission (2PPE). Up to now Co/Pt systems have attracted strong interest due to their high perpendicular magnetic anisotropy in ultrathin films. Additionally, exhibiting large magneto-optical Kerr effects they represent suitable candidates for applications in magneto-optical recording media.[9–11] Since both the exchange splitting and the spin-orbit coupling are preconditions for the appearance of magneto-optical effects the combination of ferromagnetic Co and Pt with high nuclear charge Z is promising for enhanced TPMCD asymmetries.[12]

In this paper we demonstrate a continuous increase in the TPMCD asymmetry in 1PPE and 2PPE with the film thickness. The SRT does not visibly influence the asymmetries in both cases. The behavior of the 2PPE asymmetry in dependence of the sample thickness differs from the 1PPE measurement. Moreover, the 2PPE asymmetry is larger than the asymmetry for one-photon photoemission. As figured out in Ref. 8, a direct connection between the Kerr ellipticity and the TPMCD asymmetry is predicted if TPMCD is treated in the framework of the polar magneto-optical Kerr effect. In order to check this relation, thickness-dependent measurements of the Kerr ellipticity in the polar configuration were conducted at the same wavelength (400 nm) as the 2PPE MCD measurements. The values were compared with calculated ellipticities and measured TPMCD asymmetries.

II. EXPERIMENTAL

Before deposition of Co and Pt, the W(110) single crystal was cleaned by repeated cycles of annealing and flashing. A

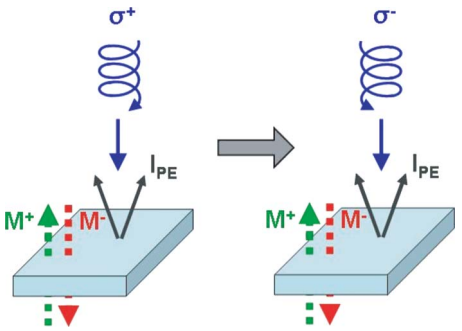

FIG. 1. (Color online) Illustration of the experimental scheme based on recording of the photoemission current I_{PE} due to irradiation with circularly polarized femtosecond laser light. The sample magnetization $\vec{M}$ is aligned parallel or antiparallel to the helicity vector of the laser beam under normal incidence to the surface.

20 ML Pt(111) buffer was afterward deposited on the substrate at a pressure of 7×10^{-9} mbar. All depositions were carried out by electron-beam evaporation at room temperature. The quality of the substrate surface and the epitaxial films was controlled by low-energy electron diffraction (LEED). The Co wedge was deposited at a pressure of 4×10^{-10} mbar by withdrawing a shutter located between the Co evaporator and the sample. The thickness along the wedge was regulated by a quartz thickness monitor. A wedge of 0–16 ML with a monolayer width of 200 μm was produced at a deposition rate of 32 s/ML. Since the formation of a Co/Pt alloy at the interface should result in increased magneto-optical signals[13,14] the sample was subsequently annealed for 11 min at a temperature of 410 °C. The structure was completed with a 15 ML thick Pt capping layer deposited at room temperature to prevent oxidation.

Frequency-doubled and frequency-tripled lights from a titanium sapphire femtosecond laser (Mai Tai, Spectra Physics, $h\nu$=4.64 eV (1PPE), $h\nu$=3.10 eV (2PPE), pulse length $\tau\sim200$ fs for the second harmonic and $\tau\sim300$ fs for the third harmonic, repetition rate 80 MHz) was used as excitation source. Photoemission was thereby excited by focusing the polarization modulated laser beam onto the sample which was placed under vacuum in the gap of a commercial electromagnet generating a homogeneous field of up to 1.12 T at the sample position. Figure 1 gives an illustration of the experimental scheme. Throughout the TPMCD experiments the sample was magnetically saturated in the out-of-plane direction, the sample magnetization $\vec{M}$ was aligned parallel or antiparallel to the helicity vector of the laser beam under normal incidence to the surface. The photoemission current of the perpendicularly magnetized film was measured by a picoamperemeter combined with a lock-in amplifier. This enables a polarization-sensitive detection of the total electron yield induced by the two helicities of circularly polarized laser light at a low signal-to-noise ratio. For detailed information about the experimental setup for the TPMCD measurements we refer to Ref. 8.

In order to determine the magnetic features of the sample Kerr measurements were conducted outside the vacuum with different electromagnets for the polar and the longitudinal setup. Polar Kerr measurements were carried out almost under normal light incidence (~5°), in the longitudinal setup *s*-polarized light with incidence angle of ~45° was chosen.

III. KERR MEASUREMENTS

Thickness-dependent Kerr measurements were conducted at room temperature in polar geometry with an external field of $\mu_0 H$=255 mT as well as in longitudinal geometry using a magnetic field of 178 mT. A focused 670 nm laser beam allowed a lateral resolution corresponding to 1 ML thickness increase on the Co wedge. As stated in Ref. 15 the complex Kerr angle,

$$\phi_K \equiv \theta_K + i\epsilon_K \tag{1}$$

consists of the Kerr rotation angle θ_K and the Kerr ellipticity ϵ_K and depends linearly on the thickness t of the investigated film on a substrate S,

$$\phi_K = \frac{i\sigma_{xy}}{\sigma_{xx}^S}\frac{4\pi t}{\lambda}, \tag{2}$$

where σ_{xx}^S is the optical conductivity of the substrate, σ_{xy} is the optical conductivity of the investigated film, and λ is the vacuum wavelength. This expression holds in the case of the polar Kerr effect and is valid when $t \ll \lambda$. With respect to Eq. (2) one would expect a linear increase in both the Kerr rotation angle and the Kerr ellipticity with increasing Co thickness. The measured values of the polar (dots) and longitudinal Kerr rotation (squares) are shown in Fig. 2(a). The polar Kerr rotation angle θ_K shows a steady increase up to 6.5 ML. At 5.5 ML the easy magnetization direction changes from out-of-plane to in-plane orientation due to the increasing shape anisotropy. At 6.5–7 ML a maximum Kerr rotation of 16.05 mdeg is reached followed by a continuous decrease since the external field does not suffice to saturate the sample magnetization in the out-of-plane direction. At the ultrathin end of the wedge the polar Kerr rotation curve exhibits a steep slope followed by a weaker increase for Co thicknesses exceeding 4 ML. In agreement with Ref. 16 these linear sections with different slopes might be attributed to a structural transition from fcc(111) to hcp(0001) Co with increasing sample thickness. Concerning the critical thickness of the spin-reorientation transition a broad range of values from 4.4 ML (Ref. 17) to 12 ML (Ref. 18) is reported in literature; a theoretical work predicts a transition at 4 ML.[19] To explain this discrepancy between the experimental and theoretical results it was demonstrated[20] that the substrate roughness affects the critical thickness of the SRT attributing an early reorientation transition to a rough substrate. In our case the Co wedge was evaporated on a 20 ML Pt buffer, which might have been rougher than a Pt single-crystal surface. This could be a reason for the SRT occurring at a relatively low Co thickness of 5.5 ML. In earlier reports a nonvanishing Kerr rotation extrapolated to zero ML Co thickness was observed and related to a polarization of Pt by neighboring Co atoms.[11] Our results in Fig. 2(a), however, show that the polar Kerr rotation increases linearly with the thickness at the ultrathin end of the wedge. There is no positive offset leading to a nonzero extrapolated Kerr rotation in agreement

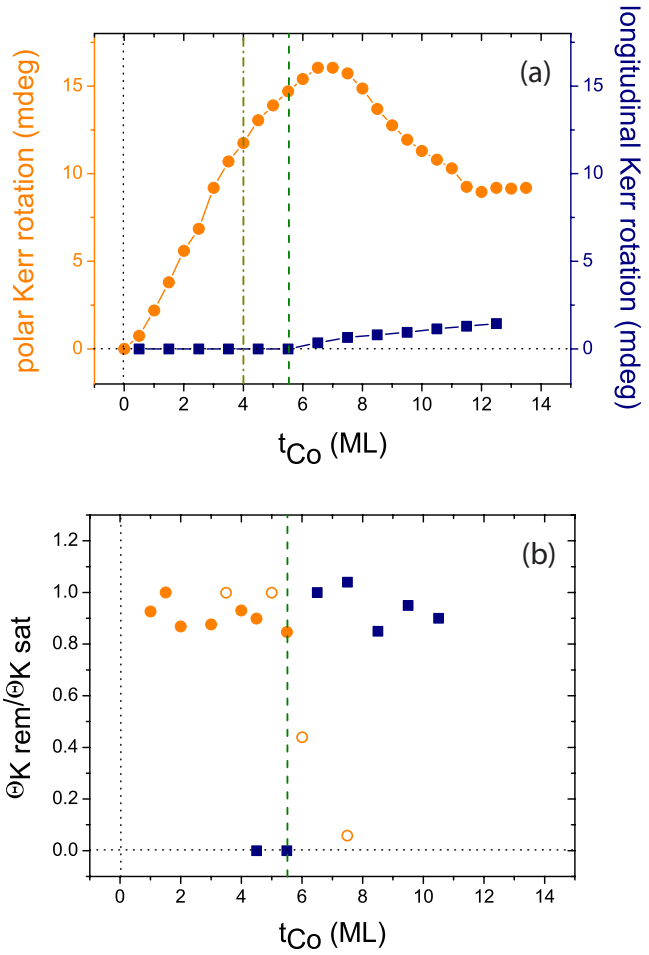

FIG. 2. (Color online) (a) Polar (dots) and longitudinal Kerr rotation angle (squares) in dependence of the Co thickness measured at external fields of 255 mT (polar setup) and 178 mT (longitudinal setup). The structural transition between fcc(111) Co and hcp(0001) Co is marked with a dashed-dotted line, the SRT is marked with a dashed line. The error bars are in the order of the symbol size. (b) Squareness $\frac{\theta_{K,rem}}{\theta_{K,sat}}$ in dependence of the Co thickness for polar (dots) and longitudinal Kerr setup (squares). The open circles correspond to data from Fig. 3 measured with higher accuracy.

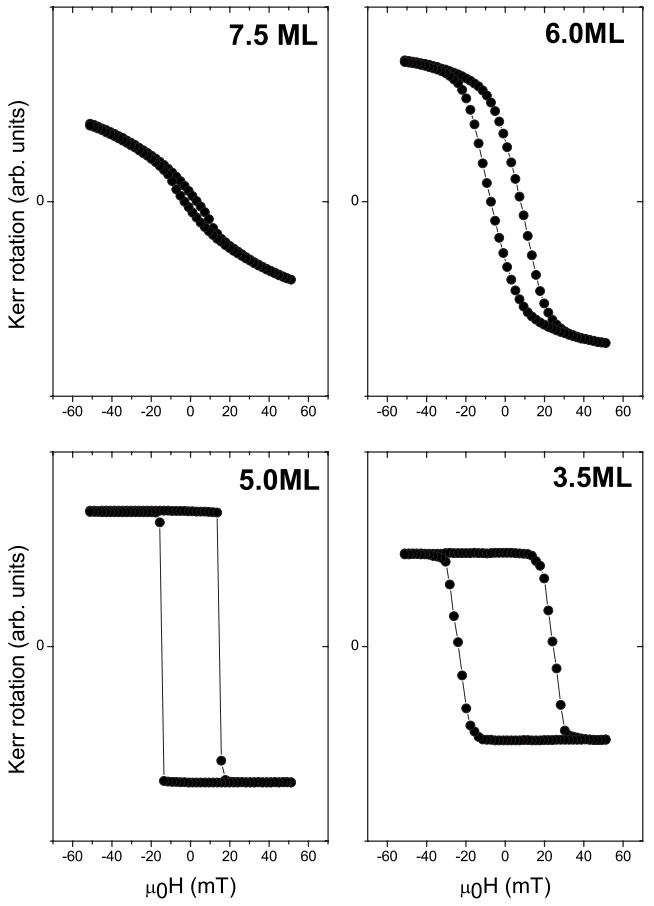

FIG. 3. Hysteresis loops for selected Co layer thicknesses measured at a maximum applied field of ±51 mT in the polar Kerr setup.

with Ref. 18. Considering that interface contributions may depend sensitively on the interface morphology[21] the extrapolated offset cannot be taken as a measure for the Pt polarization, which is certainly present. In accordance with the polar Kerr measurement the longitudinal Kerr rotation (squares) measured at an external field of 178 mT is equal to 0 up to 5.5 ML Co thickness, where it starts to increase almost linearly with the sample thickness. While in the polar setup easy axis curves are observed until a thickness of 5.5 ML, the in-plane magnetization loops show a square behavior starting from 6.5 ML. This means that the SRT takes place between 5.5 and 6.5 ML.[22]

To confirm the position of the SRT not only by the saturation values of the Kerr rotation, the squareness $\frac{\theta_{K,rem}}{\theta_{K,sat}}$ was plotted in dependence of the sample thickness [see Fig. 2(b)]. $\theta_{K,rem}$ is the remanent value while $\theta_{K,sat}$ describes the saturation value of the Kerr rotation θ_K. According to the observation of an easy axis magnetization curve the squareness in the polar case (dots) is ~1 until the SRT is reached at 5.5 ML. Subsequently, it drops rapidly since the magnetization direction has changed to an in-plane configuration. For the in-plane geometry the squareness (squares) is also ~1 in the region above the SRT and 0 beyond the SRT.

Figure 3 depicts a set of hysteresis loops for selected Co layer thicknesses measured at a maximum applied field of ±51 mT, clearly demonstrating the transition from an easy axis magnetization curve at 3.5 ML to an in-plane configuration at 7.5 ML in the polar Kerr setup.

IV. TPMCD MEASUREMENTS

TPMCD measurements were carried out at room temperature in one-photon photoemission (frequency-tripled laser light, 4.64 eV) as well as in two-photon photoemission (frequency-doubled laser light, 3.10 eV). For a sharp focusing of the incident laser beam, which is indispensable for the generation of 2PPE processes, the sample was placed in the focal point of a fused silica lens (f=15 mm), at the same time allowing monolayer thickness-sensitive detection of the TPMCD asymmetry. To ensure that in the case of 4.64 eV the excitation process is governed by one-photon photoemission, the linear dependence of the photoelectron current on

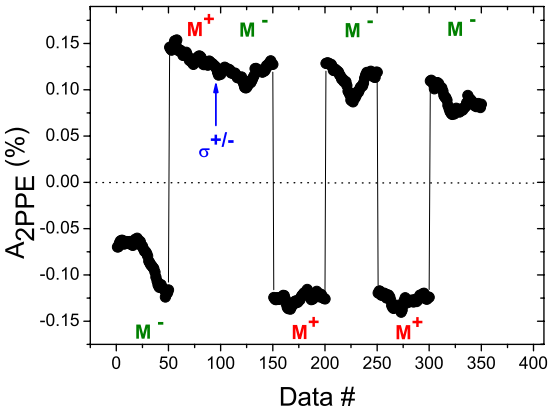

FIG. 4. (Color online) Measurement sequence for verification of the TPMCD asymmetry, based on reversals of the magnetization direction $M^{\pm}$ and changes in the photon helicity $\sigma^{\pm}$. The arrow marks a simultaneous change in the magnetization direction and the photon helicity.

the laser power was checked, simultaneously revealing that the value for the sample work function is <4.64 eV. In the case of 3.1 eV a quadratic behavior was measured indicating 2PPE processes. By means of ultraviolet photoelectron spectroscopy the sample work function was determined to $\Phi = (4.6 \pm 0.2)$ eV.

Polarization modulated laser light was used to measure asymmetries in the photoemission yield depending on the helicity relative to the magnetization vector. Figure 4 gives an example of a TPMCD asymmetry measurement in two-photon photoemission on the Co/Pt wedge, where measurement sequences are defined by magnetic field reversals together with helicity changes in the photon beam. The helicities are labeled with $\sigma^{\pm}$, corresponding to two different phase settings at the lock-in amplifier for the polarization-selective detection of the photoemission signal. TPMCD is confirmed by two criteria (1) periodic changes in the photoemission signal following periodic changes in the orientation of magnetizations M^+ and M^- parallel or antiparallel to the laser beam and (2) steadiness of the photoemission signal during a simultaneous change in both the magnetic field orientation and the helicity. In this sense, Fig. 4 verifies magnetic circular dichroism. In order to calculate the TPMCD asymmetry

$$A = \frac{\bar{I}_e^+ - \bar{I}_e^-}{\bar{I}_e^+ + \bar{I}_e^-} \approx \frac{\bar{I}_e^+ - \bar{I}_e^-}{2\bar{I}_e}, \tag{3}$$

the output voltages of the lock-in amplifier were referred to the corresponding photocurrent values I_e^+ and I_e^-, which were averaged over segments with the corresponding magnetizations M^+ and M^-. During 2PPE measurements with 3.1 eV photon energy the average laser power was 44 mW. To ensure that the thickness region with an out-of-plane magnetization is saturated on the one hand and to guarantee that the 2PPE laser spot is stable in position during the reversal of the external field on the other hand, the magnetic field was set to an intermediate value of 222 mT.

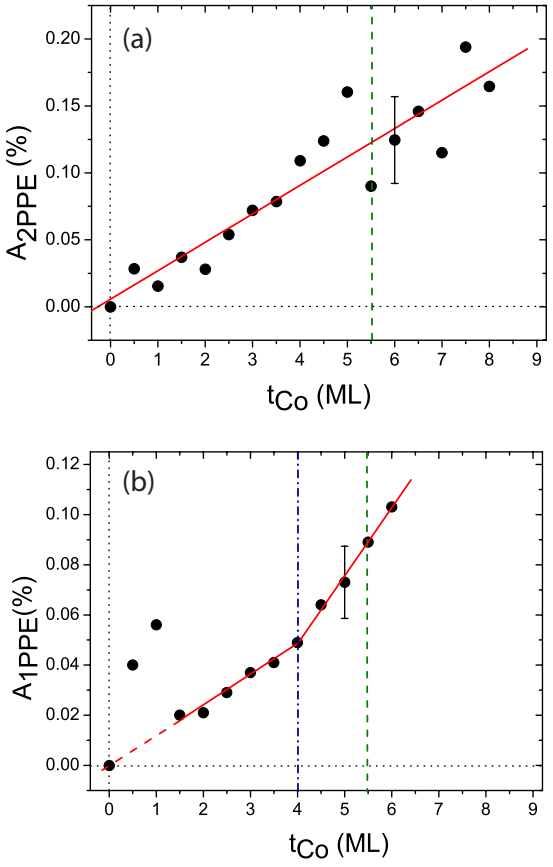

FIG. 5. (Color online) (a) 2PPE TPMCD asymmetry in dependence of the Co thickness measured at an external field of 222 mT. (b) Same for 1PPE TPMCD measured at an external field of 0.74 T. The structural transition between fcc(111) Co and hcp(0001) Co is marked with a dashed-dotted line, the SRT is marked with a dashed line. The photon energies used for 2PPE and 1PPE are 3.1 eV and 4.64 eV, respectively. All TPMCD measurements were carried out in the polar Kerr setup. For both measurements error bars for a chosen monolayer thickness have been derived and are mainly due to the dynamical behavior of the lock-in amplifier.

Figure 5(a) depicts a thickness-dependent 2PPE MCD measurement, revealing a linear increase in the asymmetry with increasing Co thickness. At 6.5 ML a value of 0.14% was recorded. As demonstrated with the Kerr data, the magnetization easy axis at 6.5 ML has changed from the out-of-plane to an in-plane direction. Obviously, an influence of the magnetization easy axis on the magnitude of the asymmetry could not be detected as the TPMCD effect increases continuously. The linear increase in the asymmetry indicates that surface effects do not play a dominant role. Otherwise a saturation of the asymmetry within the first monolayers of the wedge is expected. Therefore, the asymmetry must be dominated by the Co bulk properties.

Results for the 1PPE TPMCD are shown in Fig. 5(b). The asymmetry was measured with an external field of 0.74 T. At 4.64 eV the laser power was set to 1.4 mW. The TPMCD asymmetry also increases monotonously with increasing Co thickness. However, the behavior of the TPMCD asymmetry is not only influenced by the film thickness. In contrast to the 2PPE measurements one-photon photoemission exhibits

three distinct regions of TPMCD: at low Co coverages up to ~1.5 ML an enhanced dichroic signal is observed which is followed by a linear increase up to ~4 ML. Here, a discontinuity occurs beyond which a steeper linear increase in the TPMCD signal is measured. At 6 ML the asymmetry reaches 0.1%. It is interesting to note that the strong TPMCD signal increase at lowest Co coverages is seen exclusively in 1PPE but not in 2PPE. At these low coverages nanomagnetism due to Co island growth is prevailing and could influence the magneto-optical properties and lead to a much stronger wavelength dependence. Furthermore the two-dimensional (2D) band structure of a monolayer Co on Pt could be favorable for a high TPMCD effect. The 2D band structure of a monolayer shows no dispersion along the surface normal and at the Γ-point atomiclike behavior prevails. Both could favor a high TPMCD. However, further measurements are needed to validate these assumptions. The transition between the linear regions with different slopes occurs at ~4 ML and might be attributed to a structural change from fcc(111) to hcp(0001) Co. This transition was also observed in the polar Kerr measurements in this paper [see Fig. 2(a)]. In Ref. 16 the crystalline transformation was detected almost in the same thickness region, where fcc(111) Co was observed at thicknesses of $d<5$ ML and passed into hcp(0001) Co for thicknesses $d>6$ ML. Since this structural change does not show up in the 2PPE measurements, 1PPE seems to be more sensitive to band structure changes conditional upon changes in the crystal structure.

V. DISCUSSION

As mentioned above, TPMCD is often treated as a magneto-optical phenomenon: In this crude model the polar Kerr ellipticity as well as the TPMCD asymmetry arise from different absorption probabilities for right/left circularly polarized light. Using the Jones formalism a direct connection can be derived,[8]

$$A_{\mathrm{TPMCD}} \approx 2\epsilon_K\left(\frac{R}{1-R}\right), \tag{4}$$

where A_{TPMCD} denotes the polar TPMCD asymmetry, ϵ_K stands for the polar Kerr ellipticity, and R is the reflectivity of the investigated sample at the given wavelength. To check the validity of this assumption the 2PPE TPMCD asymmetry was compared with the Kerr ellipticity measured at 3.1 eV. By the use of an additional quarter-wave plate monolayer thickness-sensitive measurements of the Kerr ellipticity were performed at an external field of 255 mT. Figure 6 depicts the TPMCD asymmetry (full squares) and the Kerr ellipticity measurement (full dots). For direct comparison all ellipticity values are already converted referring to Eq. (4). Considering that by varying the Co thickness from 0 to 3.2 nm the reflectivity R is changed by less than 1% and keeping in mind that there is only a thickness-independent influence of the Pt capping layer a value of $R=0.75$ was used for a 15 ML Pt/(0–16) ML Co wedge on Pt at $h\nu=3.1$ eV.[23]

The polar Kerr ellipticity does not show the same behavior as the TPMCD asymmetry. Up to a thickness of ~2 ML the ellipticity steadily increases for larger Co thicknesses,

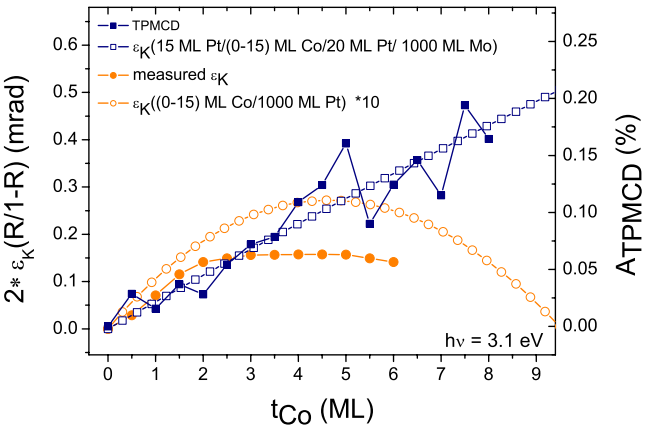

FIG. 6. (Color online) Comparison of the 2PPE TPMCD asymmetry (full squares) with the polar Kerr ellipticity measured with 3.1 eV photon energy at an external field of 255 mT (full dots) and calculated polar Kerr ellipticities for different sample systems: (open squares): 15 ML Pt/(0–15) ML Co/20 ML Pt/1000 ML Mo and (open circles): (0–15) ML Co/1000 ML Pt. The calculations were carried out for 3.1 eV. To compare the Kerr ellipticities with the TPMCD asymmetry the ellipticity values were converted according to Eq. (4). In the case of the Pt substrate the values were additionally multiplied by a factor of 10.

however, it saturates while the TPMCD asymmetry further increases. Moreover, the TPMCD signal is about one order of magnitude larger than deduced from Eq. (4). This can be attributed to a selection of energy and angular momentum in threshold photoemission leading to higher asymmetries. On the one hand for TPMCD only states in the vicinity of the Fermi level are involved while all states from E_F to $E_F-h\nu$ can participate in the excitation process in magneto-optic Kerr effect. This directly leads to an averaging over many transitions resulting in reduced Kerr signals. On the other hand momentum conservation allows only vertical transitions in the band-structure scheme because the UV photon carries only a negligible momentum. In addition, close to threshold only a narrow cone of k vectors inside the material can contribute to the electron yield. The majority of the electrons is excited outside this narrow cone and stays inside of the material due to total reflection at the surface. All these electrons contribute to photoabsorption but not to the electron yield.

Furthermore, due to the saturation effect of the measured Kerr ellipticity it does not seem to satisfy Eq. (2), predicting a linear increase with thickness. However, thickness-dependent calculations for different sample systems and photon energies reveal that ϵ_K as well as θ_K generally show a continuous increase with increasing sample thickness. Deviations from this behavior only occur for those photon energies where the Kerr signal is close to zero or even exhibits a zero crossing. The appropriate calculations were carried out by a program code based on transfer-matrix calculations.[24]

Figure 6 also depicts the thickness dependence of the calculated Kerr ellipticity for a 15 ML Pt/(0–15) ML Co/20 ML Pt/1000 ML Mo sample (open squares). Since the data for tungsten could not be incorporated in the program code, Mo was chosen to reasonably model the present sample system.

Similar to the TPMCD asymmetry the calculated ellipticity steadily increases with the sample thickness and does not show any deviations from a linear behavior. It should be noted that the polar Kerr ellipticity of this sample system is not close to zero at photon energies around 3.1 eV. For comparison ϵ_K of a (0–15) ML Co/1000 ML Pt sample was also calculated, the ellipticity values were additionally multiplied by a factor of 10 (open circles). This curve does not show the same characteristics, in contrast it resembles the shape of the measured ellipticity curve. The Co/Pt sample system exhibits a Kerr ellipticity close to zero between about 2.8 and 3.4 eV, which might be the reason for the differing behavior. Disregarding the different magnitudes of the quantities the calculated behavior corresponds to the measured Kerr ellipticity. We conclude that deviations of the Kerr ellipticity from the linear thickness dependence are connected to photon energy ranges, where the polar Kerr ellipticity is close to zero or even exhibits a zero crossing. For the present sample system the measured Kerr ellipticity deviates from a linear behavior indicating that ϵ_K might be close to zero in the vicinity of 3.1 eV. The measured values can be best compared to the calculated Kerr ellipticities for a (0–15) ML Co/1000 ML Pt wedge. If ϵ_K is not close to zero around 3.1 eV it is expected to depend linearly on the sample thickness. This is the case for the Mo substrate. Since for the same sample system and photon energy the behavior as well as the magnitude of ϵ_K in dependence of the sample thickness strongly deviates from the TPMCD asymmetry, we further conclude that Eq. (4) cannot adequately describe the relation between the Kerr ellipticity and the TPMCD asymmetry. Obviously, it does not suffice to apply the Jones formalism to threshold photoemission under the assumption that the absorbed light intensity is proportional to the total photoemission yield. In this sense, TPMCD is not sufficiently described in the framework of the magneto-optical Kerr effect. Rather, it must be taken into account that for photoemission the number of contributing transitions is strongly reduced by momentum and energy conservation. Direct insights in transitions taking place in 1PPE and 2PPE processes can be given by relativistic band-structure calculations.

In our case the band structure of hcp Co as well as for fcc Co has to be considered. The escape cone effect limits possible transitions to the normal-emission direction, i.e., $\Gamma\Lambda L$ for fcc and $\Gamma\Delta A$ for hcp. A fully relativistic band structure for fcc Co has been given in Ref. 25. In the presence of perpendicular magnetization and normal light incidence as well as normal electron emission transitions from initial states with Λ_6^3+, Λ_6^3- symmetry to final states of Λ_6^1+, Λ_6^1- symmetry mainly contribute to the dichroic signal. For the 1PPE case electrons can only stem from bands $\lesssim 0.2$ eV below E_F. Hence, a majority band of Λ_6^3- symmetry, crossing the Fermi edge at $\sim 75\%$ of the ΓL direction as well as a minority band of Λ_6^3+ symmetry with a horizontal tangent 150 meV below E_F are two candidates for the initial states with different spin character. (The value of 150 meV refers to the band-mapping measurement by Kuch *et al.*[25]) Since final states with Λ_6^1 symmetry cannot be reached by 1PPE processes the final state is an evanescent state (also called inverse LEED state) coupling to a free-electronlike parabola at the solid-vacuum interface. For 2PPE processes with an excitation energy of $2h\nu = 6.2$ eV bands $< (1.6 \pm 0.2)$ eV below E_F can contribute to the electron yield. Since all other bands in this energy range do not exhibit Λ_6^3 symmetry an excitation from the upper majority band (Λ_6^3-) and the lower minority band (Λ_6^3+) in final end states with Λ_6^1 symmetry is most likely. However, it should be noted that these considerations are based on the dipole selection rules calculated for a single electron excitation. In the present situation no real band exists in the region of the intermediate state. In such cases 2PPE is often described as a coherent process, where two photons are absorbed simultaneously.[26] This is in accordance with the model used in Ref. 2 yielding reasonable agreement with 2PPE MCD measurements of two Heusler alloys. Furthermore it should be noted that in 2PPE transitions the excess energy is 1.6 eV. Thus a large part of the valence bands may contribute in normal emission and a sizeable $k_\parallel$ range of up to 0.65 A^{-1} (i.e., 35% of the Brillouin zone) becomes accessible. For these reasons it might be more adequate to call the 2PPE excitation a *near* threshold photoemission process. Moreover, it should be mentioned that in our case excitation out of interband hybridization points in image potential states leading to circular dichroism in 2PPE as discussed in Ref. 27 is not possible.

The band structure of hcp Co along $\Gamma\Delta A$ has been calculated by Braun.[28] For the 1PPE case only minority states contribute to the dichroism. Directly at the Γ point a spin-orbit split minority band (Δ_7/Δ_9 symmetry) exhibits a high density of states and crosses the Fermi energy at $\sim 25\%$ of the ΓA direction. Since the dipole selection rules only allow transitions from Δ_7/Δ_9- to Δ_7-symmetry bands electrons from these initial states are excited to evanescent states in the case of 1PPE. For 2PPE the situation is different since also majority bands can contribute to the dichroic signal. For the excitation in real final-state bulk bands the parabolalike Δ_8 band, which sets in at about ~ 6 eV (majority band) and ~ 7 eV (minority band) may serve as final band. To this band excitation from initial bands with Δ_8/Δ_9 symmetry are allowed. For the minority channel electrons can therefore only be excited from a parabolalike Δ_8 band, which is located ~ 0.3 eV below E_F at the Γ point. However, in this case transitions might only take place under the assumption of lifetime broadening of the final state. For the majority channel transitions from the spin-orbit split Δ_8/Δ_9-symmetry band and a parabolalike Δ_8 band, which are located at ~ 0.5 eV below E_F at the Γ point, might be possible. Besides, it should be noted that the sudden increase in slope at 4 ML [see Fig. 4(b)] most likely reflects the occurrence of hcp Co bands.

Finally we have to consider the influence of the Pt cap layer. Figure 7 depicts the calculated Kerr rotation (open squares) and Kerr ellipticity (full circles) at 3.1 eV for a 5.5 ML Co/20ML Pt/1000 ML Mo sample in dependence of the Pt capping layer thickness. With increasing thickness of the capping layer the Kerr rotation decreases rapidly due to the fact that the incident light is more and more absorbed by the nonmagnetic overlayer until the ferromagnetic signal fades out at a capping thickness of about 30 nm. Assuming an exponential decrease with increasing thickness of the capping layer we determine an information depth ($1/e$ decrease) of ~ 9 nm. With a 4 nm Pt capping the Kerr rotation has

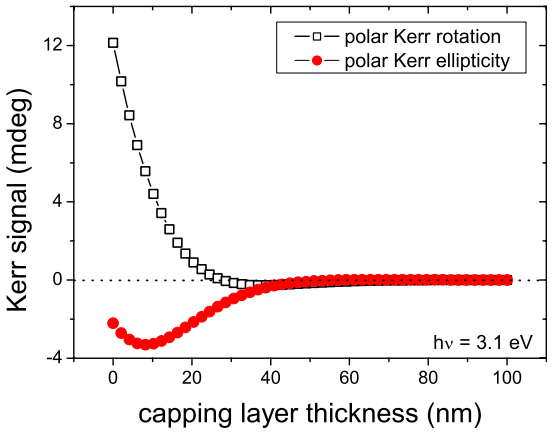

FIG. 7. (Color online) Calculated polar Kerr rotation (open squares) and polar Kerr ellipticity (full circles) in dependence of the capping layer thickness for a 5.5 ML Co /20 ML Pt/1000 ML Mo sample system. The calculation was carried out for 3.1 eV.

already decreased to 70% of the initial value and it can be assumed that this leads to a reduction in the TPMCD asymmetry, as well. Measurements of Marx *et al.*[29] have demonstrated that a cap layer (in that case Ag) substantially reduces the TPMLD asymmetry measured for a Ag/Fe/W system. While for Kerr measurements an information depth of 21.5 nm was found, a value of 16.2 nm was derived for photoemission measurements. Due to the limited mean-free path of the detected electrons TPMCD experiments are more surface sensitive than Kerr measurements. Therefore the TPMCD asymmetry will decrease more rapidly with increasing capping layer thickness, i.e., in our case the information depth of the TPMCD will be smaller than 9 nm. On the other hand, our experiments show no saturation of the TPMCD with increasing Co thickness up to 8 ML (1.6 nm). This means that the information depth of the TPMCD effect is larger than 1.6 nm. The reduction in the TPMCD asymmetry due to a cap layer arises by different reasons. Photoemission from the Pt capping will lead to a background signal that shows no MCD (except for a possible small polarization of Pt at the interface). The Pt contribution to the total signal will thus diminish the observed asymmetries. Furthermore, considerable transport losses of the Co photoelectrons occur in the cap layer that may depend on the Pt band structure. The losses do not depend on the photon helicity, so they will diminish the intensity but not the MCD asymmetry. Overall, the transport losses of the Co photoelectrons and additional intensity by the Pt photoelectrons cause a decrease in the MCD asymmetry.

In contrast to the Kerr rotation, the absolute value of the Kerr ellipticity first increases with the capping thickness until a maximum around 8 nm followed by a rapid decrease (Fig. 7). At 30 nm Pt capping the Kerr ellipticity is also nearly zero. This is interesting since the Kerr ellipticity is also expected to decrease with increasing capping layer thickness. The reason for this behavior might be found in the exact calculation of the transfer matrix based on the optical Fresnel equations.

VI. CONCLUSION

In conclusion, TPMCD in 1PPE and near TPMCD in 2PPE has been investigated for a Pt-capped Co wedge on Pt(111)/W(110). At 5 ML asymmetry values of 0.07% for 1PPE and 0.11% for 2PPE were measured. The spin-reorientation transition was found at 5.5 ML. For 2PPE as well as for 1PPE the asymmetry increases continuously with the film thickness. While in the case of 2PPE a linear dependence on the wedge thickness was found the behavior for 1PPE is more subtle. Two linear sections with different slopes were detected and attributed to different Co crystal structures. These results allow three conclusions to be drawn: (i) the basic mechanism leading to TPMCD must be connected with Co bulk properties and surface effects do not play a dominant role. (ii) An influence of the magnetization easy axis on the asymmetry for a perpendicularly magnetized film could not be detected. (iii) The comparison of the TPMCD asymmetry with measured and calculated Kerr ellipticities in the framework of the Jones formalism reveals that the relation between the TPMCD asymmetry and the Kerr ellipticity cannot be adequately described by Eq. (4). Finally, the 1PPE and 2PPE asymmetries were referred to transitions in the relativistic band-structure scheme of fcc and hcp Co and it was shown that the effective probing depth of TPMCD exceeds 1.6 nm.

ACKNOWLEDGMENTS

We would like to thank T. Nakagawa for fruitful discussions and K. Medjanik for the UPS measurements. The experiment was funded by the DFG (Grant No. EL 172/15-1), the Carl-Zeiss-Stiftung (Kerstin Hild), and the Graduate School Materials Science in Mainz (Kerstin Hild).

*hildk@uni-mainz.de

[1] G. K. L. Marx, H. J. Elmers, and G. Schönhense, Phys. Rev. Lett. **84**, 5888 (2000).
[2] K. Hild, J. Maul, G. Schönhense, H. J. Elmers, M. Amft, and P. M. Oppeneer, Phys. Rev. Lett. **102**, 057207 (2009).
[3] T. Nakagawa and T. Yokoyama, Phys. Rev. Lett. **96**, 237402 (2006).
[4] T. Nakagawa, T. Yokoyama, T. Hosaka, and M. Katoh, Rev. Sci. Instrum. **78**, 023907 (2007).
[5] T. Yokoyama, T. Nakagawa, and Y. Takagi, Int. Rev. Phys. Chem. **27**, 449 (2008).
[6] T. Nakagawa, I. Yamamoto, Y. Takagi, K. Watanabe, Y. Matsumoto, and T. Yokoyama, Phys. Rev. B **79**, 172404 (2009).
[7] C. T. Chiang, A. Winkelmann, P. Yu, and J. Kirschner, Phys. Rev. Lett. **103**, 077601 (2009).
[8] K. Hild, J. Maul, T. Meng, M. Kallmayer, G. Schönhense, H. J. Elmers, R. Ramos, S. K. Arora, and I. V. Shvets, J. Phys.: Condens. Matter **20**, 235218 (2008).

[9] W. B. Zeper, F. J. A. M. Greidanus, P. F. Carcia, and C. R. Fincher, J. Appl. Phys. **65**, 4971 (1989).
[10] S. C. Shin, Appl. Surf. Sci. **65-66**, 110 (1993).
[11] N. W. E. McGee, M. T. Johnson, J. J. de Vries, and J. aan de Stegge, J. Appl. Phys. **73**, 3418 (1993).
[12] P. M. Oppeneer, J. Sticht, T. Maurer, and J. Kübler, Z. Phys. B: Condens. Matter **88**, 309 (1992).
[13] M. T. Lin, H. Y. Her, Y. E. Wu, C. S. Shern, J. W. Ho, C. C. Kuo, and H. L. Huang, J. Magn. Magn. Mater. **209**, 211 (2000).
[14] M. T. Lin, C. C. Kuo, J. W. Ho, Y. E. Wu, H. Y. Her, C. S. Shern, and H. L. Huang, Appl. Surf. Sci. **169-170**, 231 (2001).
[15] P. Bruno, Y. Suzuki, and C. Chappert, Phys. Rev. B **53**, 9214 (1996).
[16] D. Weller, A. Carl, R. Savoy, T. C. Huang, M. F. Toney, and C. Chappert, J. Phys. Chem. Solids **56**, 1563 (1995).
[17] C. S. Shern, J. S. Tsay, H. Y. Her, Y. E. Wu, and R. H. Chen, Surf. Sci. **429**, L497 (1999).
[18] J. Kim, J.-W. Lee, J.-R. Jeong, S.-C. Shin, Y. H. Ha, Y. Park, and D. W. Moon, Phys. Rev. B **65**, 104428 (2002).
[19] U. Pustogowa, J. Zabloudil, C. Uiberacker, C. Blaas, P. Weinberger, L. Szunyogh, and C. Sommers, Phys. Rev. B **60**, 414 (1999).
[20] J. Kim, J.-W. Lee, J.-R. Jeong, S.-K. Kim, and S.-C. Shin, Appl. Phys. Lett. **79**, 93 (2001).
[21] M. Przybylski, L. Yan, J. Zukrowski, M. Nyvlt, Y. Shi, A. Winkelmann, J. Barthel, M. Wasniowska, and J. Kirschner, Phys. Rev. B **73**, 085413 (2006).
[22] H. Fritzsche, J. Kohlhepp, H. J. Elmers, and U. Gradmann, Phys. Rev. B **49**, 15665 (1994).
[23] A. Nabok and A. Tsargorodskaya, Thin Solid Films **516**, 8993 (2008).
[24] Program code based on transfer-matrix calculations, http://www.msd.anl.gov/groups/mf/jmkerrcalc.php
[25] W. Kuch, A. Dittschar, M. Salvietti, M.-T. Lin, M. Zharnikov, C. M. Schneider, J. Camarero, J. J. de Miguel, R. Miranda, and J. Kirschner, Phys. Rev. B **57**, 5340 (1998).
[26] M. Cinchetti, D. A. Valdaitsev, A. Gloskovskii, A. Oelsner, S. A. Nepijko, and G. Schönhense, J. Electron Spectrosc. Relat. Phenom. **137-140**, 249 (2004).
[27] M. Pickel, A. B. Schmidt, F. Giesen, J. Braun, J. Minar, H. Ebert, M. Donath, and M. Weinelt, Phys. Rev. Lett. **101**, 066402 (2008).
[28] M. Getzlaff, J. Bansmann, J. Braun, and G. Schönhense, J. Magn. Magn. Mater. **161**, 70 (1996).
[29] G. K. L. Marx, P.-O. Jubert, A. Bischof, and R. Allenspach, Appl. Phys. Lett. **83**, 2925 (2003).